

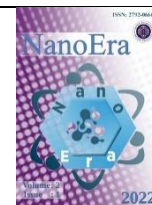
PAPER DETAILS

TITLE: Effect of nitrogen doping amount on the activity of commercial electrocatalyst used in PEM fuel cells

AUTHORS: Niyazi ÖZCELIK,Ayşe BAYRAKCEKEN YURTCAN

PAGES: 5-9

ORIGINAL PDF URL: <https://dergipark.org.tr/tr/download/article-file/2476602>



Effect of nitrogen doping amount on the activity of commercial electrocatalyst used in PEM fuel cells

Niyazi OZCELIK ¹, Ayse BAYRAKCEKEN YURTCAN ^{2, 3*}

¹ Department of Chemistry, Faculty of Science, Hacettepe University, Istanbul, Turkey

² Department of Chemical Engineering, Faculty of Engineering, Atatürk University, 25240, Erzurum, Turkey

³ Department of Nanoscience and Nanoengineering, Graduate School of Natural and Applied Sciences, Atatürk University, 25240, Erzurum, Turkey

*Corresponding author E-mail: abayrakceken@atauni.edu.tr

HIGHLIGHTS

- > Nitrogen doping was achieved on a commercial catalyst.
- > Nitrogen to catalyst ratio was changed.
- > Changing nitrogen amount altered contact angle and PEM fuel cell performance.

ARTICLE INFO

Received : 08 April 2022

Accepted : 04 June 2022

Published : 09 June 2022

Keywords:

Nitrogen Doping
Melamine
N-doped Catalyst
Contact Angle
PEM Fuel Cell

ABSTRACT

The amount of nitrogen doping has attracted attention recently because it provides additional catalytically active sites in catalysts. In this study, nitrogen-doped (N-doped) catalysts were synthesized by mixing melamine as a nitrogen source and commercial Tanaka catalyst with 67% Pt loading in different amounts of melamine. After nitrogen doping, N-doped catalysts were characterized by FTIR, XRD, elemental analysis, contact angle measurement, and PEM fuel cell performance tests. Change in the nitrogen amount in the catalyst resulted in an increase in the PEM fuel cell performance which can be attributed to the significant change in contact angle and so in the hydrophobicity of the catalysts.

1. Introduction

The Proton exchange membrane (PEM) fuel cell has received great attention due to its power efficiency, non-hazardous waste, and moderate operating conditions. Various conditions are needed to achieve high performance, such as efficient use of platinum, conductive support, and an active catalyst. In addition to all these conditions, the commercialization of the PEM fuel cell is hindered at a high cost due to the use of platinum and unstable catalysts. Many researchers have tried to reduce the amount of platinum by developing non-platinum metal catalysts or by improving durable catalysts and the electrochemical activity of platinum. Mostly, carbon-supported platinum catalysts are used as catalysts, but these catalysts have some problems such as dissolution and agglomeration of platinum [1–5].

Some researchers have tried to increase its effectiveness by modifying the supplement material, either in-situ or ex-

situ [6]. Different elements such as nitrogen, boron, fluor, and sulfur are used as additives. Nitrogen is a commonly used additive. Various chemical compounds such as melamine, pyrrole, aniline, 1,10 phenanthroline, dicyanamide, ethylenediamine, and phthalocyanine are used as nitrogen sources. Supporting nitrogen-functionalized carbon was also of interest because functionalization with nitrogen resulted in avoiding the existing 3D morphology, which facilitates aggregation and the porous channel that allows the mass transfer. Due to the increased potential of these catalysts and obtaining durable catalysts, some researchers have studied this phenomenon recently [7].

Both Pt-alloyed and nitrogen-doped hybrid supports have been studied in the literature. Reduced graphene oxide and multi-walled carbon nanotube (MWCNT) were used as hybrid support and pyrrole was used as a nitrogen source. The prepared nitrogen-containing hybrid support was annealed at 800 °C for 3 hours under an argon atmosphere. The Pt alloy was reduced compared to the hybrid support and



when all the performance results were examined, it was seen that the nitrogen-doped reinforced PtFe_3 had the best performance compared to PtCo_3 and Pt/C . These may be due to the nitrogen content in the hybrid support and the high dispersion of the alloys [8].

Nitrogen-doped graphene nanoplatelets (N-G) were prepared in situ using NH_3 as a nitrogen source. Then, the obtained support was used and Pt nanoparticles were reduced on it. Finally, the fuel cell performance of the prepared electrocatalyst was measured. After measurements, the maximum power densities of N-G and Pt/G were 440 mW/cm^2 and 390 mW/cm^2 , respectively. This difference is due to the decomposition of the intermediate of oxygen reduction reaction (ORR) by the anchor side, high conductivity, and nitrogen doping [9].

Graphene, CNT, or different ratios of Graphene and CNT were initially mixed with the ionic liquid of 1-ethyl-3-methylimidazolium dicyanamide and then pyrolyzed at 600°C for 1 minute. The fuel cell performance of the obtained electrocatalysts showed that Pt@G/N-CNT had the best current density at 0.65 V among all electrocatalysts [10].

Another study was conducted with Pt/C and ethylenediamine. Ethylenediamine was fixed on Pt/C by reflux for 8 hours at 75°C . Thus, the catalyst was coated with ethylenediamine at a thickness of 1 nm. After the anchoring process, the prepared catalyst was annealed and the annealing temperature was optimized by changing the temperature between 400 and 700°C with an increase of 100°C . It was understood that the nitrogen doping of carbon atoms causes an increase in electronegativity and this facilitates the adsorption of oxygen molecules. The available densities of the catalysts were 1804, 1788, 1555, 1521, and 1280 mA/cm^2 for the Pt/C catalyst with annealing temperatures of 400, 500, 600, and 700°C [11].

Commercial catalyst (Pt/C) was also functionalized with aniline. For this purpose, the aniline monomer was polymerized with ammonium persulfate and the resulting catalyst contains nitrogen. The performance result showed that the durability of the nitrogen-doped catalyst was higher than that of Pt/C [12].

In another study, a platinum and aniline complex was obtained in an inert medium and then heated at 500°C for 2 hours in a nitrogen atmosphere. The authors noticed that after performance measurements, Pt/C outperformed the prepared catalyst. The reason for the decrease in the performance of the prepared catalyst was attributed to the difference between the Pt/C thicknesses and the $5 \mu\text{m}$ and $50 \mu\text{m}$ values of the prepared catalyst, respectively. However, the authors showed that the prepared catalyst had better durability than Pt/C due to the carbonized aniline shell protecting them from platinum agglomeration and Ostwald ripening [13].

Nitrogen-doped CNT (N-CNT) was first prepared by chemical vapor deposition method and ethylenediamine and pyridine were used as nitrogen sources. They showed that N-CNTs synthesized with nitrogen-rich ethylenediamine showed superior catalytic activity for the ORR [14].

The sandwich structure of Pt-CNT was first prepared by annealing under ammonia gas, then the Pt NPs were reduced and the second nitrogen layer was coated by mixing the prepared Pt/N-CNT and PVP, then annealed under a nitrogen atmosphere at 500°C for 2 hours. The maximum power densities of the prepared catalysts are 676, 539, 376 mW/cm^2

for the Pt-CNT, N-CNT, and Pt/Carbon black sandwich structures, respectively. This difference may be due to the nitrogen-doped carbon layer, which contributes to the adsorption and desorption of oxygen species on the Pt surface [15].

Jung et al. studied nitrogen-doped carbon-supported Pt and PtCo catalysts and the results showed that the hybrid supports performed better than Pt/C after accelerated stress tests of the prepared catalysts [16–18].

In this work, commercially available Pt/C catalyst was doped with nitrogen using melamine as the nitrogen source. The catalyst-melamine ratios were varied to determine the effect of different nitrogen doping levels on the properties of the catalysts. The catalysts were characterized using FT-IR, XRD, and contact angle measurements. Elemental analysis was used to determine the nitrogen content. PEM fuel cell performance tests were conducted to find the catalyst with the best fuel cell performance.

2. Experimental

2.1. Synthesis of nitrogen-doped Pt/C

In order to dope nitrogen over commercial Pt/C (Tanaka, 67 %) catalysts, melamine was used as a nitrogen source. The required amounts of the catalyst and melamine depending on the targeted ratios were grained mechanically in mortar having the catalyst to melamine ratios of 1:1, 4:1, 8:1 for 10 min. After mixing, the prepared mixture was annealed at 900°C for 1 h under a nitrogen atmosphere as shown in Figure 1.

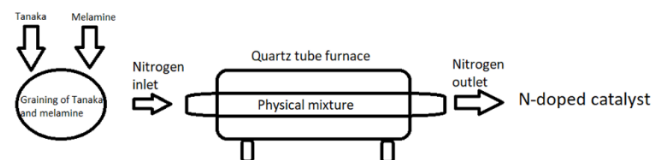


Figure 1. Representative synthesis scheme

2.2. Characterization

2.2.1. Physical characterization of Nitrogen-doped Pt/C

The nitrogen-doped catalysts were characterized by using FT-IR, XRD, contact angle measurement, and PEM fuel cell performance tests. Functional groups over the catalysts were investigated by using Fourier transform infrared spectroscopy (FT-IR) with Perkin Elmer Spectrum One. In order to identify crystal structure, XRD data were obtained by a Rigaku Miniflex X-ray diffractometer. The diffractometer with a CuK_α ($\lambda = 1.5406 \text{ \AA}$) radiation source was operated in continuous scan mode at a scan rate of $0.6^\circ \text{ min}^{-1}$ in the range of $10 - 90^\circ (2\theta)$. In order to determine the hydrophobic character of the prepared catalysts, we measured contact angle at room temperature with Attension Theta Optic Tensiometer & Topography. The nitrogen amount over the catalysts was determined by the AFK-5 elemental analysis instrument.

2.2.2. Membrane electrode assembly (MEA) preparation and fuel cell testing

In order to characterize the electrochemical activities of the prepared catalysts, in-situ PEM fuel cell performance tests were performed with a single fuel cell hardware. For the cell performance test, the membrane electrode assemblies (MEAs) were prepared by brushing catalyst ink (including definite amounts of catalyst, 2-propanol (Sigma Aldrich), and Nafion solution) onto gas diffusion layers (GDLs). The platinum loading over the electrode was set to 0.4 mg Pt cm⁻². Then, a five-layer MEA was prepared by pressing these GDLs onto the Nafion 212 membrane at 130 °C, 400 psi for 4 min in order to create a good interfacial contact between the GDL and the catalyst layer. The geometric area of the electrode was 4.41 cm². A commercially available PEM fuel cell hardware (Electrochem) and fuel cell test station (Henatech) were used for the experiments. During the experiments, the temperature of the single-cell was maintained at 70 °C, and fully humidified hydrogen/oxygen gases were fed into the anode/cathode at 70 °C at flow rates of 250 ml/min.

3. Results and Discussion

The XRD patterns are shown in Figure 2 exhibit the representative diffraction peaks at 39.8°, 46.3°, 68.2°, and 81.6°. They indicated that all the broad diffraction peaks of the XRD patterns at 2θ = 39.6, 47.4, and 67.1° corresponding to the reflections of (111), (200), (220), respectively, which are consistent with the face-centered cubic (fcc) structure of platinum (Pt) which can be assigned to (JCPDS Card 04-0802), thus demonstrating the presence of crystalline Pt.

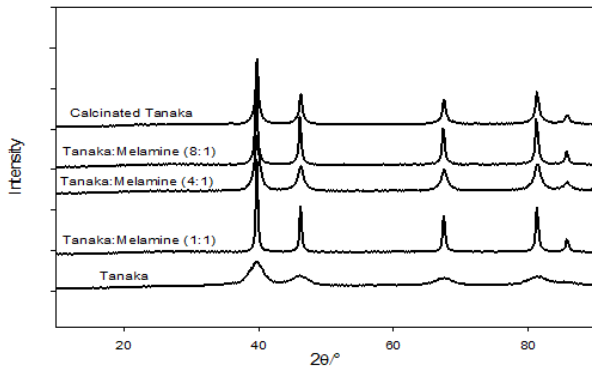


Figure 2. XRD patterns of the prepared catalysts

This indicates the presence of platinum in the catalysts. Characteristic peaks of Tanaka-Melamine (4:1) catalyst are significantly sharper than Tanaka catalyst due to the crystallite size effect. Scherer equation was used to calculate the particle sizes of the Pt nanoparticles by using the (110) plane from XRD data (Table 1).

Table 1. Particle sizes calculated from the Scherer equation

Catalyst name	Particle size (nm)
Tanaka	3.01
Tanaka: Melamine (1:1)	3.26
Tanaka: Melamine (4:1)	2.96
Tanaka: Melamine (8:1)	3.13
Calcinated Tanaka	3.85

Pt particle sizes were increased with heat treatment. The Scherrer equation (Equation 1) is given below where, L = average crystal size (angstrom or nm); B = the full-width half maximum of the peak; K = the Scherrer constant; depends on the how the width is determined, the shape of the crystal, and the size distribution; λ = the wavelength of the radiation used to collect the data.

$$L = \frac{0.9\lambda}{B\cos\theta} \quad (1)$$

Figure 3 exhibits the IR spectrums of the catalysts. The band located at nearly 1600 - 1650 cm⁻¹ can be attributed to the C=C group [19,20]. The small peak located at around 1750 cm⁻¹ is assigned to C=O (carbonyl) stretching vibration [19]. As can be seen from Figure 3, a broad N-H stretching absorption band is located between 3200-3600 cm⁻¹ [19]. The band located at nearly 2800-2950 cm⁻¹ can be attributed to C-H [20].

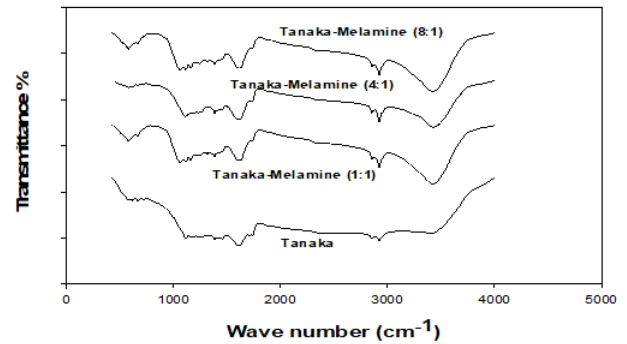


Figure 3. FT-IR spectrum of the prepared catalysts

Elemental analysis is used to determine which element is present in the structure (Table 2). In this study, we tried to dope nitrogen and used it to evaluate nitrogen amount with elemental analysis. Nitrogen amounts were determined by using elemental analysis. The amount of nitrogen increased as the amount of melamine increased and a very small amount that could not able to be detected with elemental analysis was obtained for the catalyst having the least melamine amount [10].

Table 2. Nitrogen contents of the prepared catalysts with elemental analysis

Catalyst name	Nitrogen amount (% wt.)
Tanaka-Melamine (1:1)	0.109
Tanaka-Melamine (4:1)	0.291
Tanaka-Melamine (8:1)	0.078

Contact angle value is a scale of surface wetting property and materials' hydrophobicity. The tangent angle value of any liquid droplet according to the solid surface baseline is called contact angle. The contact angle measurements were taken at room temperature (Figure 4) and are tabulated in Table 3. All the catalysts showed the hydrophobic characteristics but an increase in the nitrogen doping amount increased the contact angle values and so the hydrophobicity. An increase in contact angle is needed for better (ORR) activity because it makes it easy to remove water that forms during the ORR process. But an increase in hydrophobicity must be at a particular level and if the contact angle is above particular hydrophobicity, increasing in hydrophobicity leads to a decrease in PEM fuel cell performance [21].

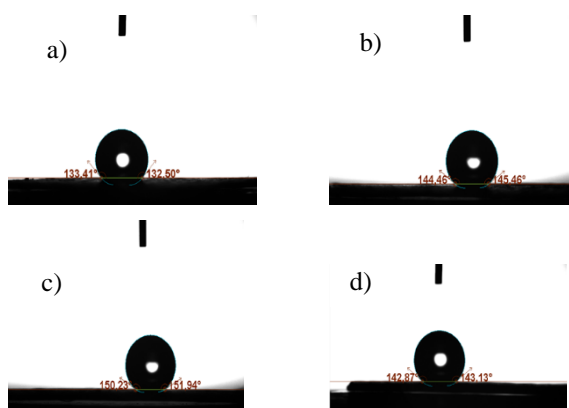


Figure 4. Contact angle measurement of the prepared catalysts a) Tanaka b) Tanaka-Melamine (4:1) c) Tanaka-Melamine (1:1) d) Tanaka-Melamine (8:1) at room temperature

Table 3. Contact angles of the prepared catalysts

Catalyst name	Contact angle
Tanaka	132.9 °
Tanaka: Melamine (1:1)	144.9 °
Tanaka: Melamine (4:1)	151.1 °
Tanaka: Melamine (8:1)	143.0 °

The performance of the PEM fuel cell is evaluated according to the typical polarization curve in which cell potential is plotted versus current density. Some degradation mechanisms occur while the cell operates so the voltage drops are seen beginning from the open-circuit voltage (OCV) to lower values along with increasing current drawn from the fuel cell. The liquid water level in the cell must be balanced for stable operation due to considerable performance loss in the event of flooding. Performances of the electrocatalysts consisting of different catalyst to melamine ratios were measured and the highest performance depending on nitrogen doping level is investigated (Figure 5). It was observed that Tanaka-Melamine (4:1) exhibited the highest current density up to higher current density values. But the further increase in the current density resulted in a decrease in the performance. From this extent of current density, Tanaka showed better performance. Calcined Tanaka catalyst which has the biggest particle size showed the worst performance result [11]. All the catalysts containing nitrogen showed concentration polarization although they had higher contact angles. These results showed that there has to be an optimum value for nitrogen doping and also contact angles.

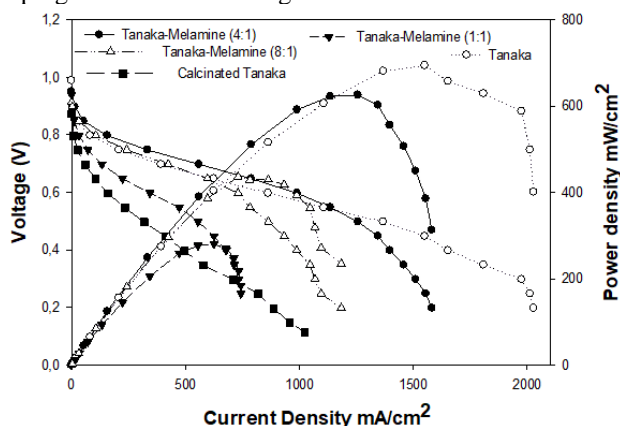


Figure 5. Polarization curve of the prepared catalysts

4. Conclusions

N-doped commercial catalysts via pyrolysis under a nitrogen atmosphere were synthesized and melamine was used as a nitrogen source due to its high nitrogen content. Nitrogen-doped catalysts were obtained and the change in the catalysts depending on the nitrogen amount is examined. When melamine was added, it was realized that contact angles differ from each catalyst significantly. It was shown that the amount of nitrogen in the catalysts has a significant impact on PEM fuel cell performance which needs to be optimized further.

Compliance with Ethical Standards

There is no conflict of interest to disclose.

Conflict of Interest

The author(s) declares no known competing financial interests or personal relationships.

Acknowledgment

The authors thank the East Anatolia High Technology Application and Research Center (DAYTAM) for the characterizations.

References

- Deng, H.; Li, Q.; Liu, J.; Wang, F. Active sites for oxygen reduction reaction on nitrogen-doped carbon nanotubes derived from polyaniline. *Carbon N. Y.* **2017**, *112*, 219–229, doi:10.1016/j.carbon.2016.11.014.
- Wang, Y.-J.; Zhao, N.; Fang, B.; Li, H.; Bi, X.T.; Wang, H. Carbon-Supported Pt-Based Alloy Electrocatalysts for the Oxygen Reduction Reaction in Polymer Electrolyte Membrane Fuel Cells: Particle Size, Shape, and Composition Manipulation and Their Impact to Activity. *Chem. Rev.* **2015**, *115*, 3433–3467, doi:10.1021/cr500519c.
- Sui, S.; Wang, X.; Zhou, X.; Su, Y.; Riffat, S.; Liu, C. A comprehensive review of Pt electrocatalysts for the oxygen reduction reaction: Nanostructure, activity, mechanism and carbon support in PEM fuel cells. *J. Mater. Chem. A* **2017**, *5*, 1808–1825, doi:10.1039/C6TA08580F.
- Shao, M.; Chang, Q.; Dodelet, J.-P.; Chenitz, R. Recent Advances in Electrocatalysts for Oxygen Reduction Reaction. *Chem. Rev.* **2016**, *116*, 3594–3657, doi:10.1021/acs.chemrev.5b00462.
- Esmailifard, A.; Rowshanzamir, S.; Eikani, M.H.; Ghazanfari, E. Synthesis methods of low-Pt-loading electrocatalysts for proton exchange membrane fuel cell systems. *Energy* **2010**, *35*, 3941–3957, doi:10.1016/j.energy.2010.06.006.
- Martínez-Huerta, M.V.; Lázaro, M.J. Electrocatalysts for low temperature fuel cells. *Catal. Today* **2017**, *285*, 3–12, doi:10.1016/j.cattod.2017.02.015.
- Du, L.; Shao, Y.; Sun, J.; Yin, G.; Liu, J.; Wang, Y. Advanced catalyst supports for PEM fuel cell cathodes. *Nano Energy* **2016**, *29*, 314–322, doi:10.1016/j.nanoen.2016.03.016.
- Vinayan, B.P.; Ramaprabhu, S. Platinum–TM (TM = Fe, Co) alloy nanoparticles dispersed nitrogen doped (reduced graphene oxide-multiwalled carbon nanotube) hybrid structure cathode electrocatalysts for high performance PEMFC applications. *Nanoscale* **2013**, *5*, 5109, doi:10.1039/c3nr00585b.
- Imran Jafri, R.; Rajalakshmi, N.; Ramaprabhu, S. Nitrogen doped graphene nanoplatelets as catalyst support for oxygen reduction reaction in proton exchange membrane fuel cell. *J. Mater. Chem.* **2010**, *20*, 7114, doi:10.1039/c0jm00467g.
- Oh, E.-J.; Hempelmann, R.; Nica, V.; Radev, I.; Natter, H. New catalyst

supports prepared by surface modification of graphene- and carbon nanotube structures with nitrogen containing carbon coatings. *J. Power Sources* **2017**, *341*, 240–249, doi:10.1016/j.jpowsour.2016.11.116.

11. Kim, H.S.; Lee, Y.; Lee, J.G.; Hwang, H.J.; Jang, J.; Juon, S.M.; Dorjgotov, A.; Shul, Y.G. Platinum catalysts protected by N-doped carbon for highly efficient and durable polymer-electrolyte membrane fuel cells. *Electrochim. Acta* **2016**, *193*, 191–198, doi:10.1016/j.electacta.2016.02.057.
12. Chen, S.; Wei, Z.; Qi, X.; Dong, L.; Guo, Y.-G.; Wan, L.; Shao, Z.; Li, L. Nanostructured Polyaniline-Decorated Pt/C@PANI Core-Shell Catalyst with Enhanced Durability and Activity. *J. Am. Chem. Soc.* **2012**, *134*, 13252–13255, doi:10.1021/ja306501x.
13. Lee, H.; Sung, Y.-E.; Choi, I.; Lim, T.; Kwon, O.J. Novel synthesis of highly durable and active Pt catalyst encapsulated in nitrogen containing carbon for polymer electrolyte membrane fuel cell. *J. Power Sources* **2017**, *362*, 228–235, doi:10.1016/j.jpowsour.2017.07.040.
14. Higgins, D.C.; Meza, D.; Chen, Z. Nitrogen-Doped Carbon Nanotubes as Platinum Catalyst Supports for Oxygen Reduction Reaction in Proton Exchange Membrane Fuel Cells. *J. Phys. Chem. C* **2010**, *114*, 21982–21988, doi:10.1021/jp106814j.
15. Zhang, Q.; Yu, X.; Ling, Y.; Cai, W.; Yang, Z. Ultrathin nitrogen doped carbon layer stabilized Pt electrocatalyst supported on N-doped carbon nanotubes. *Int. J. Hydrogen Energy* **2017**, *42*, 10354–10362, doi:10.1016/j.ijhydene.2017.02.156.
16. Jung, W.S.; Popov, B.N. Hybrid cathode catalyst with synergistic effect between carbon composite catalyst and Pt for ultra-low Pt loading in PEMFCs. *Catal. Today* **2017**, *295*, 65–74, doi:10.1016/j.cattod.2017.06.019.
17. Jung, W.S.; Popov, B.N. Improved durability of Pt catalyst supported on N-doped mesoporous graphitized carbon for oxygen reduction reaction in polymer electrolyte membrane fuel cells. *Carbon N. Y.* **2017**, *122*, 746–755, doi:10.1016/j.carbon.2017.07.028.
18. Jung, W.S.; Popov, B.N. New Method to Synthesize Highly Active and Durable Chemically Ordered fct-PtCo Cathode Catalyst for PEMFCs. *ACS Appl. Mater. Interfaces* **2017**, *9*, 23679–23686, doi:10.1021/acsami.7b04750.
19. Fraga, T.J.M.; da Silva, L.F.F.; de Lima Ferreira, L.E.M.; da Silva, M.P.; Marques Fraga, D.M. dos S.; de Araújo, C.M.B.; Carvalho, M.N.; de Lima Cavalcanti, J.V.F.; Ghislandi, M.G.; da Motta Sobrinho, M.A. Amino-Fe₃O₄-functionalized multi-layered graphene oxide as an ecofriendly and highly effective nanoscavenger of the reactive drimaren red. *Environ. Sci. Pollut. Res.* **2020**, *27*, 9718–9732, doi:10.1007/s11356-019-07539-z.
20. Groppo, E.; Bonino, F.; Cesano, F.; Damin, A.; Manzoli, M. CHAPTER 4. Raman, IR and INS Characterization of Functionalized Carbon Materials. In *Metal-free Functionalized Carbons in Catalysis*; Royal Society of Chemistry, 2018; pp. 103–137 ISBN 1757-6733.
21. Öztürk, A.; Fıçıcılar, B.; Eroğlu, İ.; Bayrakceken Yurtcan, A. Facilitation of water management in low Pt loaded PEM fuel cell by creating hydrophobic microporous layer with PTFE, FEP and PDMS polymers: Effect of polymer and carbon amounts. *Int. J. Hydrogen Energy* **2017**, *42*, 21226–21249, doi:10.1016/j.ijhydene.2017.06.202.